




ORIGINAL ARTICLE

Artificial intelligence-powered spatial analysis of tumor-infiltrating lymphocytes as a predictive biomarker for axitinib in adenoid cystic carcinoma

Dong Hyun Kim MD¹  | Yoojoo Lim MD² | Chan-Young Ock MD, PhD² | Gahee Park PhD² | Seonwook Park PhD² | Heon Song MS² | Minuk Ma MS² | Mohammad Mostafavi PhD² | Eun Joo Kang MD, PhD³  | Myung-Ju Ahn MD, PhD⁴ | Keun-Wook Lee MD, PhD⁵ | Jung Hye Kwon MD, PhD⁶ | Yaewon Yang MD, PhD⁷ | Yoon Hee Choi MD, PhD⁸ | Min Kyoung Kim MD, PhD⁹ | Jun Ho Ji MD, PhD¹⁰ | Tak Yun MD, PhD¹¹ | Sung-Bae Kim MD, PhD¹² | Bhumsuk Keam MD, PhD^{1,13} 

¹Department of Internal Medicine, Seoul National University Hospital, Seoul, South Korea

²Lunit, Seoul, South Korea

³Department of Internal Medicine, Korea University Guro Hospital, Korea University College of Medicine, Seoul, South Korea

⁴Department of Medicine, Samsung Medical Center, Sungkyunkwan University School of Medicine, Seoul, South Korea

⁵Department of Internal Medicine, Seoul National University College of Medicine, Seoul National University Bundang Hospital, Seongnam, South Korea

⁶Department of Internal Medicine, Chungnam National University College of Medicine, Daejeon, South Korea

⁷Department of Internal Medicine, Chungbuk National University Hospital, Cheongju, South Korea

⁸Department of Internal Medicine, Dongnam Institute of Radiological and Medical Sciences, Busan, South Korea

⁹Division of Hematology-Oncology, Department of Internal Medicine, Yeungnam University Hospital, Yeungnam University College of Medicine, Daegu, South Korea

¹⁰Department of Internal Medicine, Samsung Changwon Hospital, Sungkyunkwan University School of Medicine, Changwon, South Korea

¹¹Rare Cancers Clinic, Center for Specific Organs Cancer, National Cancer Center, Goyang, South Korea

¹²Department of Oncology, Asan Medical Center, University of Ulsan College of Medicine, Seoul, South Korea

¹³Cancer Research Institute, Seoul National University College of Medicine, Seoul, South Korea

Correspondence

Bhumsuk Keam, Department of Internal Medicine, Seoul National University Hospital, 101, Daehak-ro, Jongro-gu, Seoul 03080, South Korea.
Email: bhumsuk@snu.ac.kr

Funding information

AstraZeneca; Merck Sharp and Dohme; Ono Pharmaceutical; Ministry of Health & Welfare, Republic of Korea; HA22C0011

Section Editor: Nabil Saba

Abstract

Background: This study analyzed the predictive value of artificial intelligence (AI)-powered tumor-infiltrating lymphocyte (TIL) analysis in recurrent or metastatic (R/M) adenoid cystic carcinoma (ACC) treated with axitinib.

Methods: Patients from a multicenter, prospective phase II trial evaluating axitinib efficacy in R/M ACC were included in this study. H&E whole-side images of archival tumor tissues were analyzed by Lunit SCOPE IO, an AI-powered spatial TIL analyzer.

Results: Twenty-seven patients were included in the analysis. The best response was stable disease, and the median progression-free survival (PFS)

Dong Hyun Kim and Yoojoo Lim contributed equally to this study.

was 11.1 months (95% CI, 9.2–13.7 months). Median TIL densities in the cancer and surrounding stroma were 25.8/mm² (IQR, 8.3–73.0) and 180.4/mm² (IQR, 69.6–342.8), respectively. Patients with stromal TIL density >342.5/mm² exhibited longer PFS ($p = 0.012$).

Conclusions: Cancer and stromal area TIL infiltration were generally low in R/M ACC. Higher stromal TIL infiltration was associated with a longer PFS with axitinib treatment.

KEYWORDS

adenoid cystic carcinoma, artificial intelligence-analysis, axitinib, predictive biomarker, tumor-infiltrating lymphocyte

1 | INTRODUCTION

Adenoid cystic carcinoma (ACC) is a rare neoplasm that accounts for 1% of all head and neck cancer cases.¹ ACC is known to have a relatively slow growth rate.^{2,3} However, most patients with ACC eventually succumb to the disease because of the high incidence of recurrence and metastasis.³ Cytotoxic chemotherapy can be considered in these patients, but inconsistent and generally poor response rates and toxicities are the major limitations.^{4,5}

Vascular endothelial growth factor (VEGF) is highly expressed in ACC, and its expression correlates with poor prognosis.^{6,7} VEGF receptor (VEGFR), platelet-derived growth factor receptor, and fibroblast growth factor receptor have all been considered as potential therapeutic targets, and drugs targeting them have been evaluated in numerous trials. Several single-arm studies of multitargeted tyrosine kinase inhibitors (TKI) including lenvatinib, regorafenib, and sunitinib have shown some effects.^{8–11} Recently, the first randomized phase II trial of axitinib in recurrent or metastatic (R/M) ACC demonstrated a substantial progression-free survival (PFS) benefit with a median PFS of 10.8 months.¹²

However, predictive biomarkers are needed for the optimal use of TKIs. To date, several studies have been conducted on the predictive genomic markers of TKI, but the results are inconsistent.^{12,13} It has been reported that tumor-infiltrating lymphocytes (TIL) evaluated by Lunit SCOPE IO, an artificial intelligence (AI)-powered analyzer of TIL, can predict prognosis according to the use of immune checkpoint inhibitors in multiple cancer types.^{14–16} Given that antiangiogenic agents have an immunomodulatory ability,^{17,18} we hypothesized that TIL might be a good predictive biomarker of axitinib. We conducted this study to analyze the predictive value of AI-powered TIL analysis in patients with R/M ACC treated with axitinib.

2 | MATERIALS AND METHODS

2.1 | Participants and study design

In this prospective collateral biomarker analysis, we obtained data from a phase II trial that assessed the efficacy of axitinib¹² in R/M ACC. This trial was an investigator-initiated, randomized, open-label, prospective phase II trial. Specific details of the study design and results of this trial have been previously published.¹² Briefly, patients with pathologically confirmed R/M ACC who had experienced disease progression within 9 months prior to the study were eligible for inclusion. Sixty patients were enrolled and randomly assigned to either the axitinib or observation arm in a 1:1 ratio. For the observation arm, patients were crossed over to axitinib treatment when disease progression was confirmed. In the axitinib arm, axitinib was administered orally until disease progression or unacceptable toxicity was observed.

The patients included in this study were part of the aforementioned phase II trial that assessed the efficacy of axitinib on ACC. Of the 60 patients, only those with hematoxylin and eosin (H&E)-stained archival tumor tissues were eligible for inclusion. The TIL density was obtained by analyzing the H&E slides of patients with Lunit SCOPE IO.

This study was conducted in accordance with the Declaration of Helsinki and the Good Clinical Practice guidelines. The study protocol was approved by the institutional review boards of the participating institutions. Written informed consent was obtained from all patients prior to participation.

2.2 | Procedures

Lunit SCOPE IO is an AI-powered spatial TIL analyzer that identifies and quantifies TIL within the cancer epithelium (CE) and stroma (CS). Lunit SCOPE IO was

trained and validated with a $13.5 \times 10^9 \mu\text{m}^2$ area and 6.2×10^6 TILs from 17 849 H&E whole-slide images (WSI) of 23 cancer types, annotated by 104 board-certified pathologists. H&E images of head and neck squamous cell carcinoma from The Cancer Genome Atlas (TCGA-HNSC) were used for comparative analysis of TIL densities.

Lunit SCOPE IO divided the WSI into CE and CS areas and counted the number of TIL in each area separately. Using this procedure, the TIL density (per 1 mm^2) of the CE or CS area was obtained. In addition, for spatial analysis of heterogeneous TIL distribution in WSI of various sizes, Lunit SCOPE IO divided WSI into 1 mm^2 -sized grids, and calculated TIL density in the CE and CS areas. The immune phenotype (IP) of each grid was defined as follows: inflamed—grids having TIL density in the total CE area of $>200/\text{mm}^2$; immune-excluded—grids having TIL density in the CS area of $>200/\text{mm}^2$ and TIL density in the CE area of $<200/\text{mm}^2$; and immune-desert—grids having TIL density $<200/\text{mm}^2$ both in the CE and CS areas. The TIL threshold of $200/\text{mm}^2$ used for IP definition was determined and updated agnostic of tumor types prior to this study, as the optimal level that predicts higher interferon- γ -responsive gene signature levels in a set of TCGA pan-carcinoma tumor samples ($N = 7454$).^{19,20} The inflamed score (IS), immune-excluded score (IES), and immune-desert score (IDS) of the WSI were defined by the number of grids annotated to a certain IP divided by the total number of grids analyzed in the WSI. Finally, the representative IP for each WSI was defined as inflamed IP if the IS was $>33.3\%$, immune-excluded IP if IES was $>33.3\%$ and IS was $>33.3\%$, and immune-desert IP if otherwise.

Moreover, next-generation sequencing (NGS) was conducted on patients who provided informed written consent. NGS was performed using the FoundationOne CDx assay, which could detect indels, copy-number alterations, rearrangements, and tumor mutational burden. Detailed information on the NGS methods was previously published.¹²

2.3 | Statistical analysis

Categorical variables between the two groups were compared using Fisher's exact test or the chi-square test, and p -values were two-sided. Differences in means or medians for continuous variables between the two groups were assessed using the Wilcoxon rank-sum test. The cut-off for discriminating between low and high TIL and IP score levels was defined as the point with the lowest p value for PFS by the log-rank test for all possible levels for each biomarker. The Kaplan–Meier method was used

TABLE 1 Baseline characteristics

| Characteristics | Total $N = 27$ |
|---|----------------|
| Age, median (range), years | 61 (30–81) |
| Sex, male, n (%) | 15 (55.6) |
| ECOG PS, n (%) | |
| 0 | 13 (48.1) |
| 1 | 14 (51.9) |
| Relapsed or metastatic, n (%) | |
| Relapsed | 10 (37.0) |
| Metastatic | 17 (63.0) |
| Disease distribution at the time of enrollment, n (%) | |
| Locoregional disease only | 0 (0) |
| Distant metastasis | 27 (100) |
| Prior RT, n (%) | 22 (81.5) |
| Number of prior systemic treatments, n (%) | |
| 0 | 6 (22.2) |
| 1 | 14 (51.9) |
| 2 or more | 7 (25.9) |
| Lung metastasis at axitinib use, n (%) | 25 (92.6) |
| Liver metastasis at axitinib use, n (%) | 2 (7.4) |
| Analyzed tissue, n (%) | |
| Primary tumor (initially surgically resected) | 23 (85.2) |
| Metastatic tumor (lung metastasis) | 4 (14.8) |
| Initially assigned group, n (%) | |
| Axitinib arm | 15 (55.6) |
| Placebo arm followed by axitinib | 12 (44.4) |

Abbreviations: ECOG PS, Eastern Cooperative Oncology Group Performance status; RT, radiation therapy.

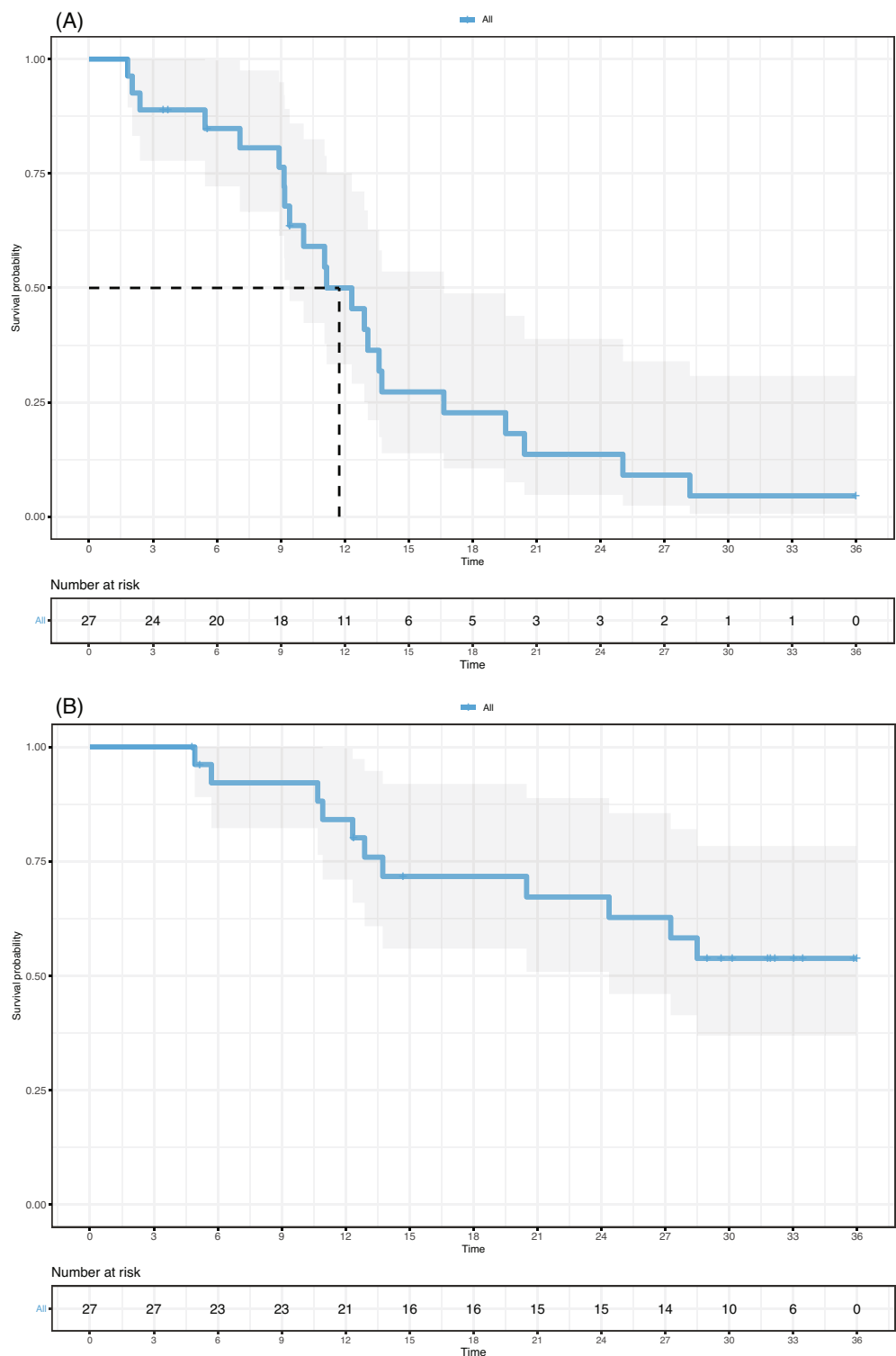
to estimate PFS and overall survival (OS). The log-rank test was used to assess differences between the groups in terms of PFS or OS. The statistical software “R” version 4.1.3 (www.r-project.org) was used for all statistical analyses. p -values of <0.05 were considered statistically significant.

3 | RESULTS

3.1 | Patient and disease characteristics

A total of 27 patients for whom H&E slides were available for analysis were included in this study. Among them, 15 and 12 patients were randomized to the axitinib group and the observation group, respectively. All 12 patients who were initially assigned to the observation arm were crossed over to axitinib after confirmed disease progression with a median PFS of 1.7 months

FIGURE 1 Survival outcomes with axitinib. (A) Kaplan–Meier curves of progression-free survival (PFS) after axitinib treatment. (B) Kaplan–Meier curves of overall survival (OS) after axitinib treatment



(95% confidence interval [CI], 0.9–4.2 months) in the observation period. The PFS with axitinib after progressive disease in the observation group was analyzed.

The demographic and baseline characteristics are shown in Table 1. The median age was 61 years (range, 30–81), and 15 patients (55.6%) were men. A total of 22 (81.5%) patients had received prior radiation therapy and 22.2% of patients had not received any prior systemic treatment.

3.2 | Efficacy of axitinib

The response to axitinib was evaluated in 27 patients. The best response to axitinib was stable disease in 25 (92.6%) patients and progressive disease in the remaining two (7.4%). More than half of the patients experienced tumor shrinkage (16 of 27, 59.3%). The 12-month PFS rate was 45.4% (95% CI, 29.0%–71.1%), with a median

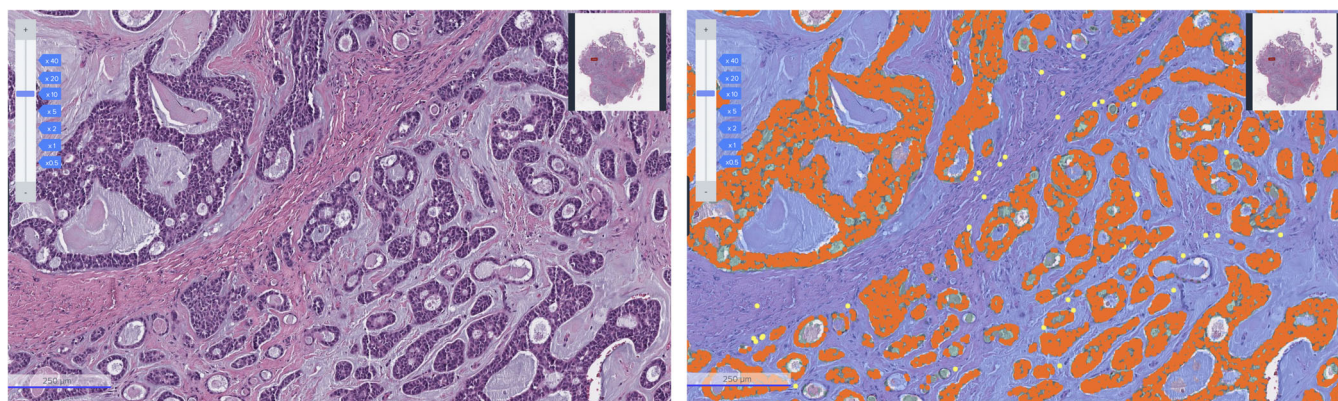


FIGURE 2 Representative image of Lunit SCOPE IO. Representative image of H&E original image (left) and Lunit SCOPE IO-inferenced segmentation of cancer epithelium (orange), cancer stroma (blue), and TIL (yellow), respectively (right)

TABLE 2 Immune phenotypes

| Phenotypes | Total N = 27 |
|---|---------------------|
| Cancer area TIL density (/mm ²), median (range) | 25.8 (0.5–462.1) |
| Stromal TIL density (/mm ²), median (range) | 180.4 (12.5–1177.1) |
| Immune phenotype score (%), median (range) | |
| Inflamed | 3.3 (0–38.2) |
| Immune-excluded | 15.6 (0–60.0) |
| Immune desert | 80.2 (20.0–100.0) |
| Immune phenotype, n (%) | |
| Inflamed | 1 (3.7) |
| Immune-excluded | 7 (25.9) |
| Immune desert | 19 (70.4) |

Abbreviation: TIL, tumor-infiltrating lymphocytes.

follow-up of 27.3 months. The median PFS was 11.1 months (Figure 1A; 95% CI, 9.2–13.7 months). The 12-month OS rate was 80.1% (95% CI, 65.9%–97.4%). However, the median OS was not determined (Figure 1B).

3.3 | TIL density analyzed by Lunit SCOPE IO

The results of the analysis by Lunit SCOPE IO are presented in Figure 2 and Table 2. The median TIL densities in the 27 patients were 25.8/mm² (interquartile range [IQR], 8.3–73.0) in the cancer area and 180.4/mm² (IQR, 69.6–342.8) in the surrounding stroma, which were lower than those in TCGA-HNSC (81.3/mm² [IQR, 43.8–172.3] and 1351.4/mm² [IQR, 658.1–2588.0], respectively). Using the log-rank test,

the optimal cut-off threshold for high and low stromal TIL density was determined to be 342.5/mm². Using this threshold, eight (29.6%) patients were in the high-stromal TIL group and the remaining 19 (70.3%) patients were in the low-stromal TIL group. The patients with a higher stromal TIL density (>342.5/mm²) exhibited longer PFS with axitinib (Figure 3A; median PFS 13.7 vs. 10.1 months, $p = 0.012$). The difference in PFS detected during axitinib treatment was not observed during the observation period in the 12 patients who were initially allocated to the observation arm. The median OS was numerically greater in patients with higher stromal TIL density (Figure 3B; not reached vs. 27.4 months, $p = 0.21$). Contrary to stromal TIL, an adequate threshold for TIL density in cancer areas could not be determined.

3.4 | Immune-excluded score and clinical outcomes of axitinib

For spatial analysis of TIL distribution, we determined the IP of each 1 mm² grid. The median IS, IES, and IDS in this cohort were 3.3, 15.6, and 80.2%, respectively. Interestingly, more than 70% (20 of 27) of the samples predominantly harbored immune-desert IP (>50% of WSI); 70% (19 of 27) of the patients had immune-desert IP, whereas only one patient had inflamed IP.

To clarify whether IP is also a predictive biomarker of axitinib treatment like stromal TIL density, we analyzed the treatment outcomes of axitinib according to either the IP or IES scores. PFS and OS were not significantly different according to IP, but differed according to IES. Median PFS was 13.7 months (95% CI, 10.1 months—not reached) in patients with a high IES (>15.8%; $n = 13$) and 11.1 months (95% CI, 7.1 months—not reached) in patients with a low IES

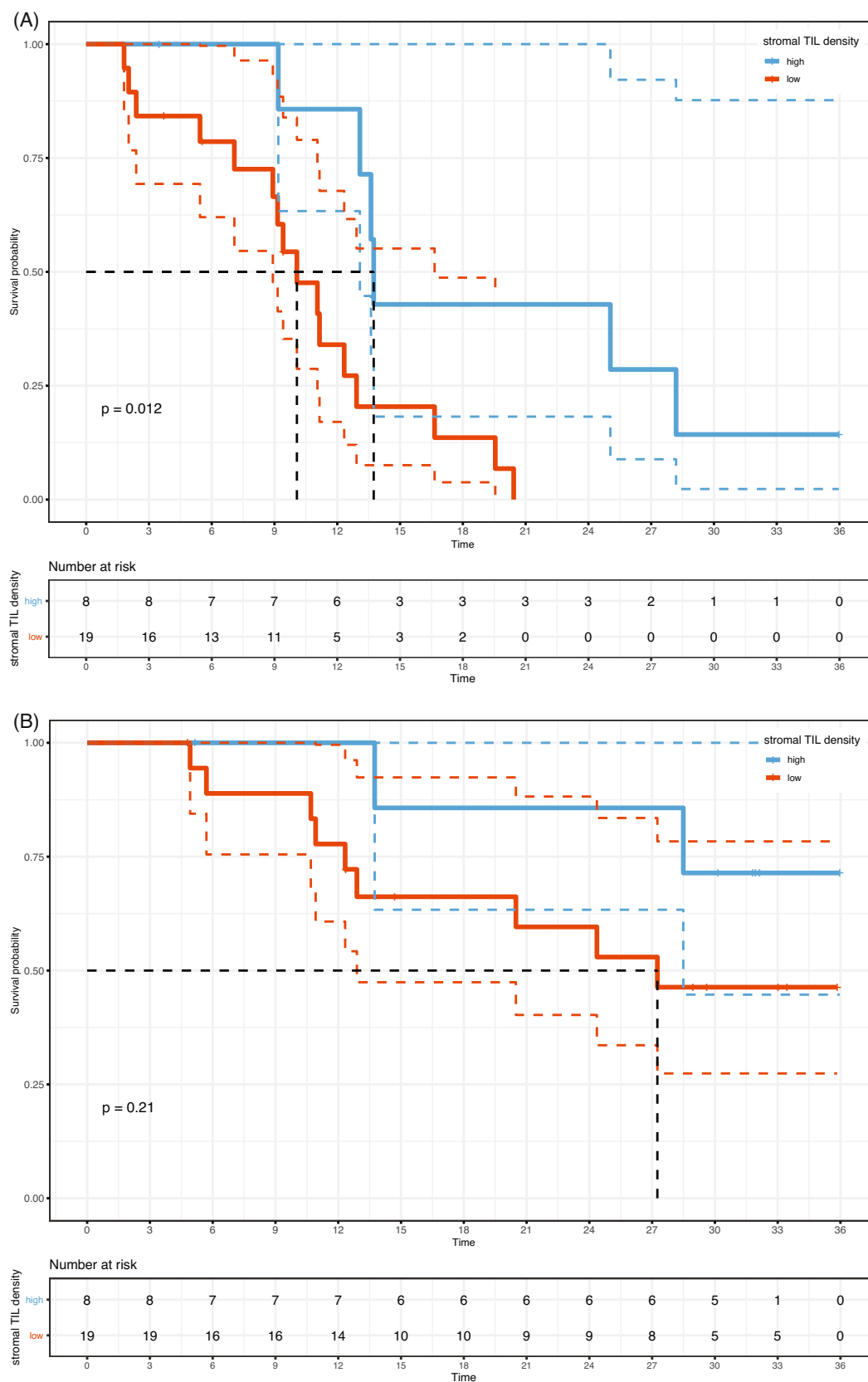


FIGURE 3 Survival outcomes with axitinib based on stromal tumor-infiltrating lymphocytes (TIL) density. (A) Kaplan-Meier curves of progression-free survival (PFS) after axitinib treatment based on stromal TIL density. (B) Kaplan-Meier curves of overall survival (OS) after axitinib treatment based on stromal TIL density

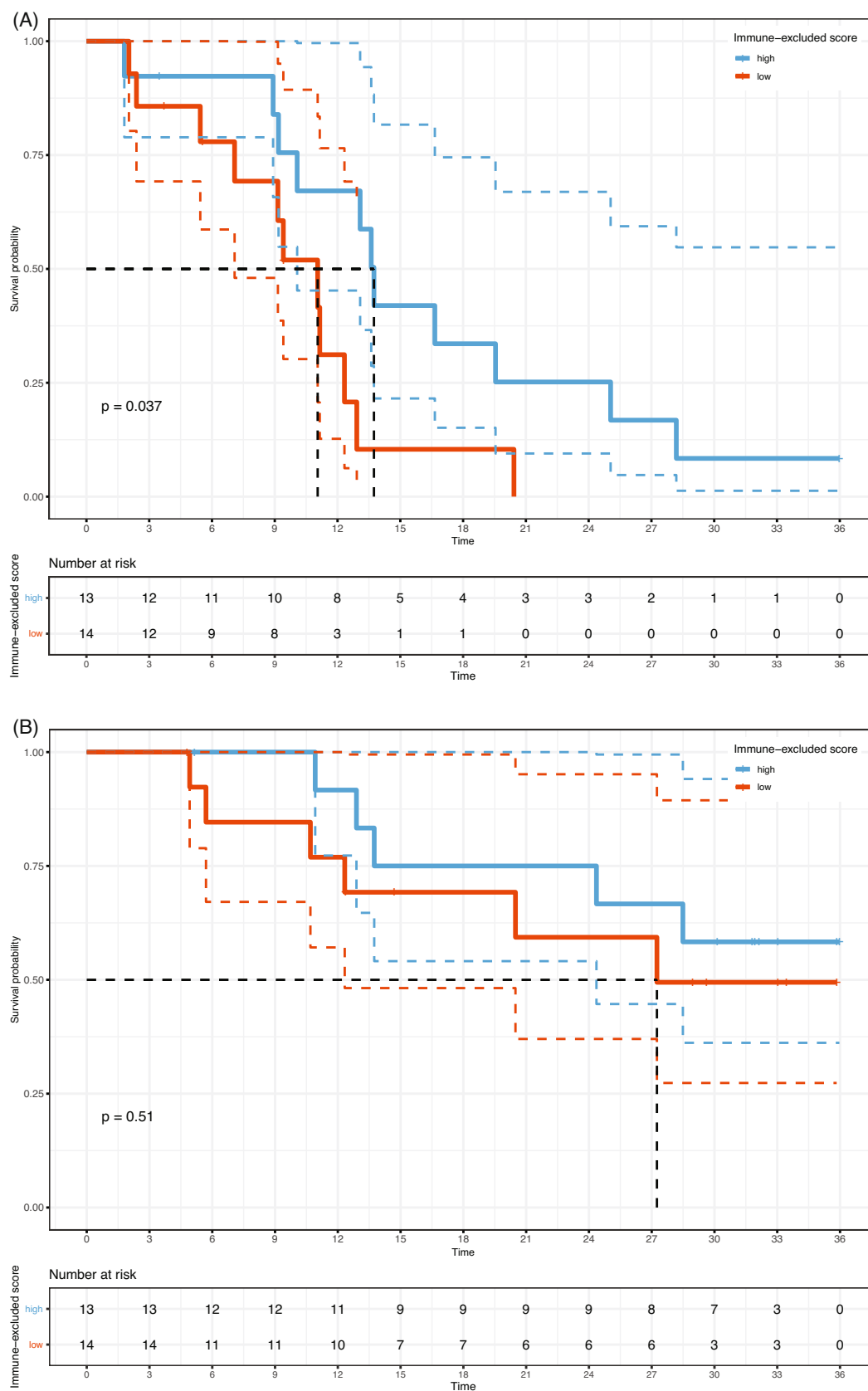


FIGURE 4 Survival outcomes with axitinib based on immune excluded score (IES). (A) Kaplan–Meier curves of progression-free survival (PFS) after axitinib treatment based on IES. (B) Kaplan–Meier curves of overall survival (OS) after axitinib treatment based on IES

($\leq 15.8\%$, $n = 14$, $p = 0.037$; Figure 4A). The median OS was numerically greater in the patients with high IES ($>15.8\%$) (Figure 4B; not reached vs. 27.4 months, $p = 0.51$).

3.5 | Genomic analysis

NGS using FoundationOne CDx assay was conducted on the pre-axitinib archival tissue samples in 22 out of the 27 patients. Integrated genomic analysis of mutations observed in three or more patients is shown in Figure S1, Supporting Information. The mutation burden for each patient ranged from 4 to 19 mutations per megabase. The most frequently identified mutations were in *KDM6A* and *ARID1B* (6/22, 27.3%), followed by *PARP4* (5/22, 22.7%). The mutation burden was not correlated with both cancer area TIL density and stromal TIL density.

4 | DISCUSSION

This study showed that (1) ACC is an immune desert cancer represented by low TIL density in both the CE and CS areas, (2) higher stromal TIL infiltration is associated with longer PFS with axitinib treatment.

Our data are consistent with those of previous studies that showed that ACC is a cancer with low immunogenicity, using immunohistochemistry.^{21–23} It has been reported that immune checkpoint inhibitors are not effective in ACC, which may be in part a result of low immunogenicity.^{24,25} The level of TIL expression is not suitable as a predictive biomarker for immunotherapy in ACC, possibly due to a similar cause.²² In a previous study analyzing TIL patterns in ACC, it was reported that the IP, represented by the spatial distribution of TIL, has no clear association with clinical outcomes.²³ Our analysis found that the IP in ACC was not associated with PFS with axitinib use. This may be because the existing classification of IP is not suitable for ACC since the TIL infiltration of the cancer area of ACC is generally low, and there is little difference between them. Instead, we found that a high proportion of immune-excluded IP was correlated with better PFS in patients with ACC treated with axitinib. A more appropriate immunophenotypic classification of ACC with low immunogenicity should be developed in the future.

Effective treatment strategies for R/M ACC are lacking. Several molecules, including MYB and VEGFR, may be potential therapeutic targets for ACC treatment.^{26,27} Based on this, the efficacy and safety of various multitargeted TKIs have been studied and some results have been achieved. There have been steady efforts to identify predictive biomarkers of TKI to identify patients who are

sensitive to TKI. However, despite several attempts, including next-generation sequencing, no predictive genomic biomarkers have been identified to guide the use of TKIs in ACC. In a previous study, starting with the rationale that MYB might be a central driver, no association between MYB expression and clinical outcome was reported.¹³ It has also been reported that the NOTCH1 mutation or amplification of 4q12 can be potential predictive biomarkers of TKI,^{8,13} but NOTCH1 is a poor prognostic biomarker.²⁸

The present study demonstrates the usefulness of TIL analyzed by Lunit SCOPE IO, an AI-powered spatial analyzer, as a novel biomarker that can optimize the use of axitinib in patients with ACC. As this study is based on the rationale that TIL might be a predictive biomarker of axitinib in patients with R/M ACC because antiangiogenic multitargeted TKIs also have an immunomodulatory ability, stromal TIL density analyzed by Lunit SCOPE IO can also act as a predictive biomarker for other TKIs such as lenvatinib, regorafenib, and sunitinib. Future studies with other TKIs and a sufficient number of patients are warranted.

This study had several limitations. The first was the small number of patients analyzed. However, given the rarity of ACC and the paucity of other studies on predictive biomarkers when using TKI, we believe that the small number of patients does not eliminate the significance of our study. Second, the AI-powered Lunit SCOPE IO has not yet been validated in ACC. Although it was developed and validated by the analysis of multiple cancer types, further validation in ACC is required. Also, the AI-powered Lunit SCOPE IO does not provide additional cellular characterization of TILs. However, it has the advantage of direct application from H&E slides without the need for additional staining, simplifying procedures and making it applicable in many cases. Third, most of the tumor tissues assessed were initially surgically resected. Needle biopsy after recurrence was not sufficient to evaluate the entire tumor microenvironment. It is possible that assessment using the initially resected tissue in the R/M setting may be a confounder. However, recent study have suggested that there may not be significant differences in the immune microenvironment between primary and metastatic tumors.²⁹ In addition, a study analyzing lung cancer with Lunit SCOPE IO used primary resected lung tissue and found that tumor microenvironment did not change much at recurrence, suggesting that it could be used to evaluate R/M settings.¹⁵

Despite these limitations, our study is the first to identify a predictive biomarker of anti-angiogenic agents for patients with R/M ACC. It is important to identify the first imaging biomarker for antiangiogenic agents. Lunit SCOPE IO can assess whole tumor tissue with a single

H&E slide in a short time, and we, therefore, believe that it will be useful and practical in clinical settings.

5 | CONCLUSION

Tumor stromal TIL density analyzed by Lunit SCOPE IO can be a predictive biomarker of axitinib in patients with R/M ACC. Patients with a higher stromal TIL density ($>342.5/\text{mm}^2$) or higher IES had a longer PFS with axitinib. Further investigations are needed to validate the value of AI-powered spatial analysis of TIL as a predictive biomarker for axitinib and other antiangiogenic TKIs in R/M ACC.

ACKNOWLEDGMENTS

This study was supported by the National R&D Program for Cancer Control through the National Cancer Center (NCC) funded by the Ministry of Health & Welfare, Republic of Korea (HA22C0011). Also, we appreciate Dr. Wonkyung Jung for pathologic review.

CONFLICT OF INTEREST STATEMENT

Bhumsuk Keam received research funding from MSD, AstraZeneca, and Ono Pharmaceutical Co., Ltd., and has served as an advisor for Handok, NeoImmuneTec, Trialinformatics and ImmuneOncia outside of the current work. Yoojoo Lim, Chan-Young Ock, Gahee Park, Seonwook Park, Heon Song, Minuk Ma and Mohammad Mostafavi are employees of Lunit, Inc., and own stocks and/or stock options of Lunit Inc.

DATA AVAILABILITY STATEMENT

The datasets generated during the current study are available from the corresponding author on reasonable request.

ORCID

Dong Hyun Kim  <https://orcid.org/0000-0002-0369-5763>

Eun Joo Kang  <https://orcid.org/0000-0003-0702-3400>

Bhumsuk Keam  <https://orcid.org/0000-0001-8196-4247>

REFERENCES

1. Renehan A, Gleave E, Hancock B, Smith P, McGurk M. Long-term follow-up of over 1000 patients with salivary gland tumours treated in a single centre. *J Br Surg*. 1996;83(12):1750-1754.
2. Jaso J, Malhotra R. Adenoid cystic carcinoma. *Arch Pathol Lab Med*. 2011;135(4):511-515.
3. Dodd R, Slevin NJ. Salivary gland adenoid cystic carcinoma: a review of chemotherapy and molecular therapies. *Oral Oncol*. 2006;42(8):759-769.
4. Papaspyrou G, Hoch S, Rinaldo A, et al. Chemotherapy and targeted therapy in adenoid cystic carcinoma of the head and neck: a review. *Head Neck*. 2011;33(6):905-911.
5. Ha H, Keam B, Ock C-Y, Heo DS. Efficacy of cyclophosphamide, doxorubicin, and cisplatin for adenoid cystic carcinoma, and their relationship with the pre-chemotherapy tumor growth rate. *Chin Clin Oncol*. 2020;9(2):15.
6. Zhang J, Peng B, Chen X. Expressions of nuclear factor κ B, inducible nitric oxide synthase, and vascular endothelial growth factor in adenoid cystic carcinoma of salivary glands: correlations with the angiogenesis and clinical outcome. *Clin Cancer Res*. 2005;11(20):7334-7343.
7. Keam B, Kim SB, Shin SH, et al. Phase 2 study of dovitinib in patients with metastatic or unresectable adenoid cystic carcinoma. *Cancer*. 2015;121(15):2612-2617.
8. Tchekmedyan V, Sherman EJ, Dunn L, et al. Phase II study of lenvatinib in patients with progressive, recurrent or metastatic adenoid cystic carcinoma. *J Clin Oncol*. 2019;37(18):1529-1537.
9. Ho AL, Sherman EJ, Baxi SS, et al. Phase II study of regorafenib in progressive, recurrent/metastatic adenoid cystic carcinoma. *J Clin Oncol*. 2016;34:6096.
10. Guigay J, Fayette J, Even C, et al. PACSA: phase II study of pazopanib in patients with progressive recurrent or metastatic (R/M) salivary gland carcinoma (SGC). *J Clin Oncol*. 2016;34:6086.
11. Chau N, Hotte S, Chen E, et al. A phase II study of sunitinib in recurrent and/or metastatic adenoid cystic carcinoma (ACC) of the salivary glands: current progress and challenges in evaluating molecularly targeted agents in ACC. *Ann Oncol*. 2012;23(6):1562-1570.
12. Kang EJ, Ahn M-J, Ock C-Y, et al. Randomized phase II study of axitinib versus observation in patients with recurrent or metastatic adenoid cystic carcinoma treatment of axitinib in adenoid cystic carcinoma. *Clin Cancer Res*. 2021;27(19):5272-5279.
13. Ho A, Dunn L, Sherman E, et al. A phase II study of axitinib (AG-013736) in patients with incurable adenoid cystic carcinoma. *Ann Oncol*. 2016;27(10):1902-1908.
14. Shen J, Lee T, Hwang J-E, et al. Artificial intelligence-powered spatial analysis of tumor-infiltrating lymphocytes predicts survival after immune checkpoint inhibitor therapy across multiple cancer types. *J Clin Oncol*. 2021;39:2607.
15. Park S, Ock C-Y, Kim H, et al. Artificial intelligence-powered spatial analysis of tumor-infiltrating lymphocytes as complementary biomarker for immune checkpoint inhibition in non-small-cell lung cancer. *J Clin Oncol*. 2022;40(17):1916-1928.
16. Jung HA, Park KU, Cho S, et al. A phase II study of nivolumab plus gemcitabine in patients with recurrent or metastatic nasopharyngeal carcinoma (KCSG HN17-11). *Clin Cancer Res*. 2022;28(19):4240-4247.
17. Hirsch L, Flippot R, Escudier B, Albiges L. Immunomodulatory roles of VEGF pathway inhibitors in renal cell carcinoma. *Drugs*. 2020;80(12):1169-1181.
18. Lapeyre-Prost A, Terme M, Pernot S, et al. Immunomodulatory activity of VEGF in cancer. *Int Rev Cell Mol Biol*. 2017;330:295-342.
19. Ayers M, Lunceford J, Nebozhyn M, et al. IFN- γ -related mRNA profile predicts clinical response to PD-1 blockade. *J Clin Invest*. 2017;127(8):2930-2940.
20. Chen DS, Mellman I. Elements of cancer immunity and the cancer-immune set point. *Nature*. 2017;541(7637):321-330.
21. Mosconi C, de Arruda JAA, de Farias ACR, et al. Immune microenvironment and evasion mechanisms in adenoid cystic carcinomas of salivary glands. *Oral Oncol*. 2019;88:95-101.

22. Chen W, Fung AS, McIntyre JB, et al. Assessment of tumour infiltrating lymphocytes and Pd-I1 expression in adenoid cystic carcinoma of the salivary gland. *Clin Invest Med*. 2021;44(1): E38-E41.
23. Doescher J, Meyer M, Arolt C, et al. Patterns of tumor infiltrating lymphocytes in adenoid cystic carcinoma of the head and neck. *Cancer*. 2022;14(6):1383.
24. Cohen RB, Delord JP, Doi T, et al. Pembrolizumab for the treatment of advanced salivary gland carcinoma: findings of the phase 1b KEYNOTE-028 study. *Am J Clin Oncol*. 2018; 41(11):1083-1088.
25. Fayette J, Even C, Digue L, et al. NISCAHN: A phase II, multicenter nonrandomized trial aiming at evaluating nivolumab (N) in two cohorts of patients (pts) with recurrent/metastatic (R/M) salivary gland carcinoma of the head and neck (SGCHN), on behalf of the Unicancer Head & Neck Group. *J Clin Oncol*. 2019;37:6083.
26. Mitani Y, Li J, Rao PH, et al. Comprehensive analysis of the MYB-NFIB gene fusion in salivary adenoid cystic carcinoma: incidence, variability, and clinicopathologic significance MYB-NFIB fusion in salivary adenoid cystic carcinoma. *Clin Cancer Res*. 2010;16(19):4722-4731.
27. Stephens PJ, Davies HR, Mitani Y, et al. Whole exome sequencing of adenoid cystic carcinoma. *J Clin Invest*. 2013;123(7): 2965-2968.
28. Ferrarotto R, Mitani Y, Diao L, et al. Activating NOTCH1 mutations define a distinct subgroup of patients with adenoid cystic carcinoma who have poor prognosis, propensity to bone and liver metastasis, and potential responsiveness to Notch1 inhibitors. *J Clin Oncol*. 2017;35(3):352-360.
29. Chang H, Kim JS, Choi YJ, et al. Overexpression of PD-L2 is associated with shorter relapse-free survival in patients with malignant salivary gland tumors. *Onco Targets Ther*. 2017;10:2983-2992.

SUPPORTING INFORMATION

Additional supporting information can be found online in the Supporting Information section at the end of this article.

How to cite this article: Kim DH, Lim Y, Ock C-Y, et al. Artificial intelligence-powered spatial analysis of tumor-infiltrating lymphocytes as a predictive biomarker for axitinib in adenoid cystic carcinoma. *Head & Neck*. 2023;45(12): 3086-3095. doi:[10.1002/hed.27537](https://doi.org/10.1002/hed.27537)